Experimental verification of line- and band-shape asymmetry in the Schumann–Runge system of O 2

M. Kono, B. R. Lewis, K. G. H. Baldwin, and S. T. Gibson

Experimental verification of line- and band-shape asymmetry in the Schumann–Runge system of O_2

M. Kono, B. R. Lewis, K. G. H. Baldwin, and S. T. Gibson

Research School of Physical Sciences and Engineering, The Australian National University, Canberra, ACT, 0200, Australia

High-resolution, laser-based photoabsorption cross-section measurements in the weakly absorbing windows between the (11,0) and (16,0) Schumann–Runge bands of O_2 have been performed at liquid-nitrogen temperature and the results compared with corresponding coupled-channel Schrödinger-equation (CSE) and line-by-line model calculations. While the symmetric-line-shape-based line-by-line model cross sections differ significantly from experiment, the excellent agreement found between the CSE and experimental window cross sections serves to confirm clearly for the first time the CSE-model predictions of band shape asymmetry and quantum-mechanical interference effects, especially in the (11,0)–(14,0) band region. © *2003 American Institute of Physics.* [DOI: 10.1063/1.1574512]

I. INTRODUCTION

The Schumann–Runge (SR) bands of O_2, $B\,^3\Sigma_u^- \leftarrow X\,^3\Sigma_g^-(v,0)$ (175–205 nm), are of central importance to the photochemistry of the terrestrial atmosphere. Photodissociation of O_2 in the SR bands is a fundamental driver of ozone formation in the middle atmosphere, while SR-band opacity controls the atmospheric penetration of solar vacuum ultraviolet (VUV) radiation.

The complex SR-band spectrum of O_2 results in the absorption of solar VUV radiation over a wide range of altitudes. Thus, proper description of this process requires knowledge of absolute photoabsorption cross sections over a range of wavelengths and temperatures. Furthermore, in order to study atmospheric photochemical processes which occur primarily over restricted wavelength ranges, it is necessary to have access to *high-resolution* photoabsorption and photodissociation cross sections, since predissociation line widths in the SR bands span a range from ~ 4 cm^{-1} full-width at half-maximum (FWHM) to well under 0.1 cm^{-1} FWHM.[1,2] As it is impractical to obtain experimental cross sections for the full range of applicable atmospheric conditions, some form of SR-band modeling is required. This has traditionally involved the development of line-by-line models,[3–7] culminating in the high-resolution, temperature-dependent polynomial model of Minschwaner *et al.*,[8] which covers the range 49 000–57 000 cm^{-1} (175–204 nm), on a 0.5 cm^{-1} grid, for temperatures of 130–500 K. Such models, each based on the best experimental data available at the time, and all assuming that the B-state predissociation can be represented by the symmetric Lorentzian line shape, have contributed much to an understanding of the photochemical implications of VUV photoabsorption and photodissociation in the SR bands.

It has been suggested recently,[9] however, in a theoretical study using the coupled-channel Schrödinger-equation (CSE) technique and a physically based SR-band model, that quantum-mechanical interference affects the magnitude of the cross section in the "window" regions of low absorption between adjacent vibrational bands. Since these regions correspond to the deeper penetration of solar VUV radiation into the middle atmosphere, such interference effects have the potential to influence the atmospheric photochemistry at those lower altitudes. These effects result in SR line- and band-shape asymmetry,[10] the consequences of which have been investigated, e.g., for the case of NO photodissociation in the middle and upper atmosphere, by Minschwaner and Starke.[11] However, the experimental evidence for band-shape asymmetry has either been indirect, or somewhat tenuous. It has been pointed out elsewhere[9] that there is a need for further measurements, concentrating on the SR cross-section windows, in order to resolve this matter.

In this work, we present new measurements of SR-band window cross sections, obtained using VUV laser-spectroscopic techniques, which provide the first convincing experimental evidence demonstrating band-shape asymmetry in the SR system. Our cross sections support the CSE-based SR-band model,[9] which inherently includes the effects of quantum-mechanical interference, rather than the traditional Lorentzian-based line-by-line models, which do not.

II. EXPERIMENT

The experimental setup was essentially the same as that described in detail elsewhere.[1,12] Briefly, coherent, tunable VUV light was generated by a two-photon-resonant four-wave difference-frequency mixing technique in Xe gas (~ 40 Torr), using two dye lasers (Lambda Physik FL3002 E) pumped by a XeCl excimer laser (Lambda Physik EMG 201 MSC). The output of one dye laser, fitted with an intra-cavity étalon, was frequency doubled by a BBO (β-Ba_2O_4) I crystal, yielding 256-nm light, which was two-photon resonant with Xe $6p[5/2]_2$, while the other, without an étalon, was varied between 465 and 442 nm, resulting in VUV generation in the wavelength range 176.6–180.1 nm, with a bandwidth ~ 0.3 cm^{-1} FWHM. On leaving the Xe cell into

which the dye-laser beams were focused, the resultant VUV radiation was separated from the non-VUV light by a 0.2 m scanning monochromator (Acton Research VM502) and was then divided by a beam splitter in order to monitor the incident VUV intensity. The transmitted VUV beam was introduced into an ~10 cm long O_2 absorption cell chilled to liquid nitrogen (LN2) temperature (effective cell temperature 79 K). The intensities of the incident (I_{mon}) and transmitted (I_{det}) beams were measured using solar-blind photomultiplier tubes (EMI 9413) and gated integrators (EG&G Princeton 4422).

In order to account for shot-to-shot variations and slow drifts of the laser intensities during a wavelength scan, in each set of cross-section measurements, I_{mon} and I_{det} were measured under the empty-cell condition (I_{mon}^0, I_{det}^0), the full-cell condition (I_{mon}^1, I_{det}^1), and the empty-cell condition again (I_{mon}^2, I_{det}^2). Then, for each wavelength, the photoabsorption cross section σ (cm^2) was determined using the Beer–Lambert law, i.e.,

$$\sigma = -\frac{1}{nl} \ln\left(\frac{2 I_{det}^1 / I_{mon}^1}{I_{det}^0/I_{mon}^0 + I_{det}^2/I_{mon}^2} \right), \tag{1}$$

where n (cm^{-3}) and l (cm) are the number density of oxygen in the absorption cell and the cell length, respectively, and all intensities have been corrected for the effects of scattered radiation. To improve the precision of the measurements, our final cross sections were determined as averages of the values obtained in at least 5 scans, each performed with signal averaging over 10 laser shots for each wavelength point. Wavelength calibration was performed using the SR-band wave numbers of Yoshino et al.[13]

The measurements were taken at LN2 temperature in order to minimize the effects of rotational smearing, which increases the window cross sections, tending to obscure the effects of the quantum-interference-induced asymmetry being studied here. All wavelength scans were performed at an O_2 pressure in the range 75–100 Torr, to minimize the statistical uncertainties in the weak window cross sections. For valid comparisons with theoretical calculations, it was necessary to correct for the effects of pressure on the cross sections. This was achieved by directly measuring the pressure coefficients at selected wavelengths in the window regions, using signal averaging over 1000 laser shots for each pressure point. Subsequently, the 75–100 Torr scans were corrected to zero pressure using pressure coefficients obtained by linear interpolation for wavelengths between those used for the direct experimental determinations. It should be noted that this procedure will *undercorrect* the cross sections in the more strongly absorbing regions of the bands where the rotational lines are more closely spaced, due to underestimating the local pressure broadening effects. However, in the windows, which are of primary interest in this work, there are not expected to be any significant systematic errors.

III. THEORY

The CSE-theoretical techniques and SR model employed here have been described in detail elsewhere.[14] Briefly, predissociation of the $B\,^3\Sigma_u^-$ state of O_2 is treated in terms of
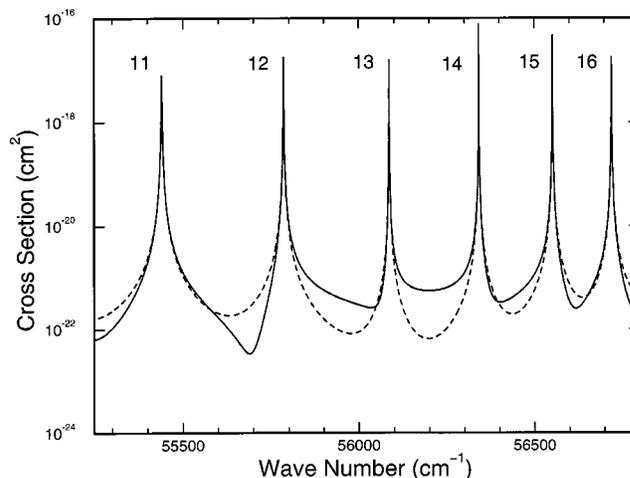

FIG. 1. Comparison between rotationless SR-band cross sections computed using the CSE (solid curve) and Lorentzian line-by-line (dashed curve) methods. Peaks are labeled according to the vibrational quantum number of the $B\,^3\Sigma_u^-$ state.

spin–orbit interactions with repulsive $^1\Pi_u$, $^3\Pi_u$, $^5\Pi_u$, and $^3\Sigma_u^+$ states, together with rotational interaction with the $^3\Pi_u$ state. The coupled-channel radial wave function for these interacting excited states is computed by solving the diabatic-basis CSE,[15,16] while the corresponding photoabsorption cross section is determined by numerical quadrature, using the coupled-channel excited-state wave function, the radial wave function of the $X\,^3\Sigma_g^-$ state, and the $B-X$ electronic transition moment.[14] The model parameters employed, i.e., the potential-energy curves, couplings, and electronic transition moment, described in Ref. 14, were determined by careful comparison with available experimental information on SR line positions, oscillator strengths, and predissociation line widths.

SR cross sections were computed[17] as a function of energy for the isotopomers $^{16}O_2$ and $^{16}O^{18}O$, for the case of zero rotation, and also full rotational spectra corresponding to a temperature of 79 K. The 79 K cross section for normal O_2 was formed by weighting the $^{16}O_2$ and $^{16}O^{18}O$ cross sections in the natural-abundance ratio 0.995 92:0.004 08. The computed cross sections inherently include the effects of SR-continuum absorption from rotationally excited X-state levels,[14,18] but exclude the effects of underlying absorption due to transitions into other states.[19]

IV. RESULTS AND DISCUSSION

In Fig. 1, the zero-rotation CSE cross section for $^{16}O_2$ in the region of the (11,0)–(16,0) SR bands (solid curve) is compared with a corresponding line-by-line model cross section taken from Ref. 9 (dashed curve). As concluded by Lewis et al.,[9] relatively high window cross sections, coupled with large relative differences between the CSE and line-by-line cross sections, make this spectral region the best candidate for experimental verification of the predictions of either model. Hence, this defines the region of interest in this work. In particular, as would be expected, the line-by-line model predicts a *minimum* window cross section between the (13,0) and (14,0) bands, the two *narrowest* bands in this region.[20] In
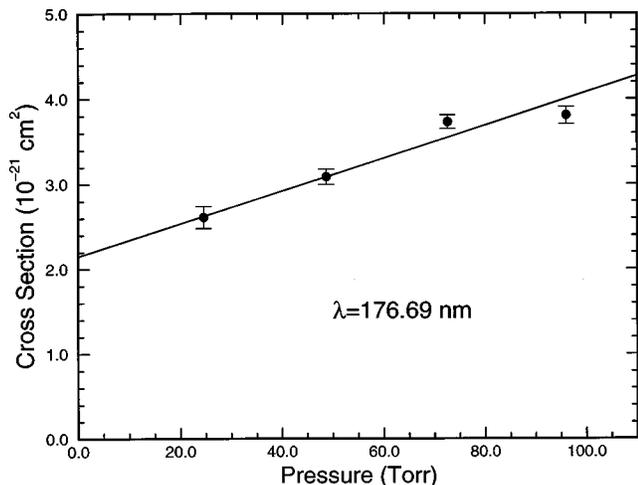
FIG. 2. $T=79$ K pressure dependence of the SR cross-section minimum near $\lambda = 176.69$ nm. Solid circles: experimental results. Solid line: linear fit to experimental results; intercept $2.15(12)\times10^{-21}$ cm^2, slope $1.93(25)$ $\times10^{-23}$ cm^2/Torr.

contrast, the CSE model predicts a *maximum* window cross section in this region, due to a constructive quantum-interference effect between these two bands. Furthermore, the CSE model predicts a very strong asymmetry (see, e.g., Ref. 10) for the (12,0) band, as opposed to the relatively symmetric band shape implied by the line-by-line model.

Experimental cross sections in the corresponding window regions were found to vary approximately linearly with O_2 pressure, as has been reported elsewhere.[21] The pressure dependence found at 176.69 nm (56597 cm^{-1}), e.g., is illustrated in Fig. 2. Cross sections, extrapolated to zero pressure, determined here for fixed wavelengths near several reference cross-section minima spanning the energy range of interest, shown in Fig. 3(a) (solid circles), are in excellent agreement with previous LN2-temperature results (crosses), obtained using a lower-resolution (~ 1.3 cm^{-1} FWHM)
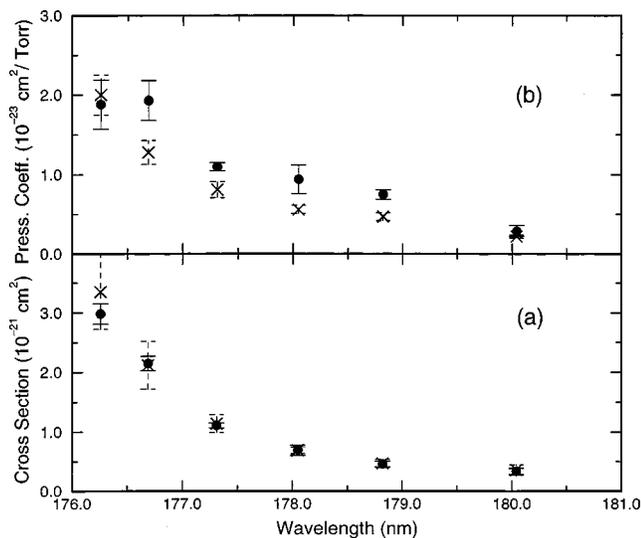

FIG. 3. (a) Experimental cross sections, extrapolated to zero pressure, at several reference minima in the SR bands. Solid circles: This work. Crosses: Ref. 21. (b) Corresponding pressure coefficients. Solid circles: This work. Crosses: Ref. 21.
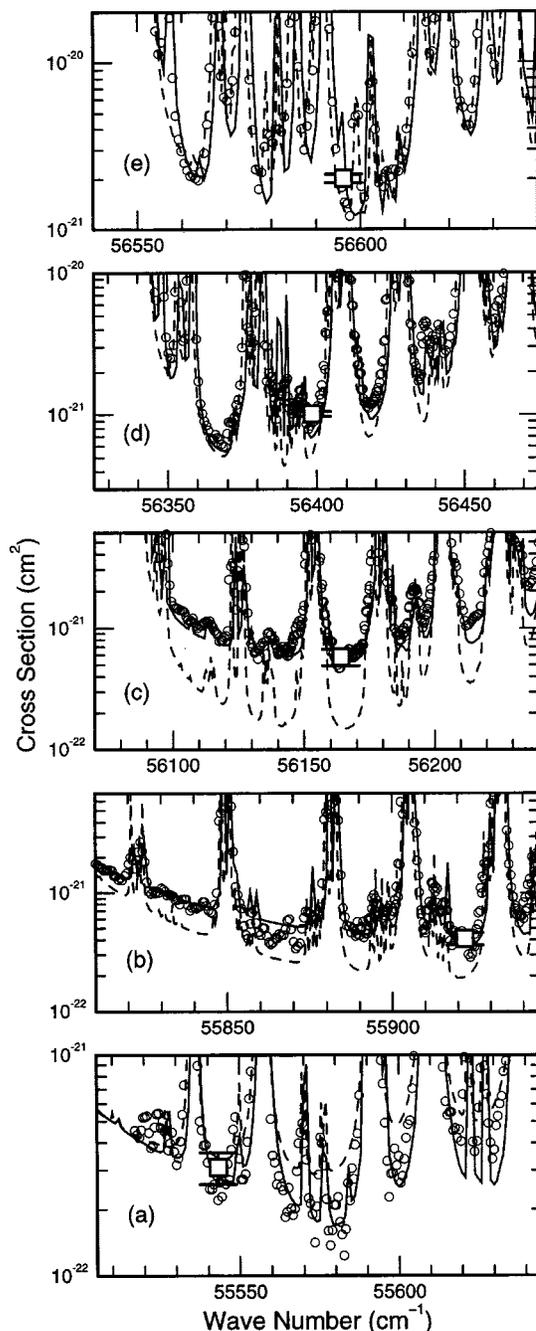

FIG. 4. Energy-dependent $T=79$ K cross sections in the vicinity of SR $(v,0)-(v+1,0)$ inter-band minima. The experimental results (open circles) have been extrapolated to zero pressure, three-point averaged, and corrected for the effects of non-SR underlying continua, allowing comparison with SR-model calculations obtained using the CSE (this work, solid curves) and Lorentzian line-by-line (Refs. 8, 23, dashed curves) techniques. The individual cross sections of Fig. 3(a), corrected as above, are shown as open squares. (a) (11,0)–(12,0). (b) (12,0)–(13,0). (c) (13,0)–(14,0). (d) (14,0)–(15,0). (e) (15,0)–(16,0).

monochromator-based system.[21] For the most part, however, the present pressure coefficients, shown in Fig. 3(b) (solid circles), exceed those of Ref. 21 (crosses).

In Fig. 4, the present energy-dependent experimental 79 K cross sections in the windows between the (11,0)–(16,0) SR bands (open circles) are compared with the corresponding predictions of the present CSE model (solid curves) and

those of the line-by-line model of Minschwaner *et al.*[8] (dashed curves). The experimental cross sections, extrapolated to zero pressure as described in Sec. II, have also been corrected downwards to allow for the effects of non-SR underlying continua. For this purpose, the *theoretical* continuum of Ref. 19 was employed, which has the advantage of being an *independent* determination, insensitive to any SR-model assumptions.[22] This correction ranges from ~ 0.3–1.5×10^{-22} cm^2, increasing with increasing transition energy, and has only a minor influence. The resulting "pure-SR" experimental cross section provides a valid comparison with the CSE-model results, which include only SR contributions, and with the line-by-line model results,[8] which have been provided to us[23] free of the contributions of underlying continua.[24]

Overall, it is clear from an examination of Figs. 4(a)–4(e) that the CSE-model cross sections are in much better agreement with the experimental results than are the line-by-line cross sections, especially in Figs. 4(a)–4(c), corresponding to the (11,0)–(14,0) inter-band windows. Particularly striking is the behavior of the wings of the (12,0) band, where both the experimental and CSE cross sections are significantly lower than line-by-line result in the low-energy wing [Fig. 4(a)], and significantly higher in the high-energy wing [Fig. 4(b)]. Thus, the experimental results support the existence of the quantum-mechanical interference-induced band-shape asymmetry predicted previously,[9,10] since the line-by-line model is predicated on the symmetric Lorentzian predissociation line shape. A previous, partially successful attempt to illustrate this asymmetry relied on the (12,0) LN2 cross section of Yoshino *et al.*,[25] which had not been intended to define the window cross sections with any precision.

The largest relative discrepancy between the CSE and line-by-line 79 K cross sections occurs in the window between the (13,0) and (14,0) bands, in the 56 150 cm^{-1} region, just as found for the rotationless case in Fig. 1. The excellent agreement between the experimental and CSE window cross sections in Fig. 4(c) thus supports the CSE prediction of a strong constructive quantum interference between the (13,0) and (14,0) transition amplitudes in this region, contrary to the intuitive expectation that, since these are the narrowest transitions in this general region, as mentioned in Sec. III, that there should be a very deep window here. Indeed, the line-by-line model echoes this expectation, predicting a deep window, since it assumes symmetric line shapes and has no mechanism to account for interference effects.

The relative performances of the CSE and line-by-line band models are summarized in Fig. 5, where the ratios of the model and experimental cross sections are plotted for the *deepest* cross-section minima in the range of the (11,0)–(16,0) SR bands. Whereas the CSE:experimental ratios (solid circles) are within 13% of unity in all cases,[26] the line-by-line:experimental ratios (crosses) range between 0.26 and 1.76. We note, however, that both the CSE and line-by-line models are capable of excellent agreement with experiment in the more strongly absorbing band regions (see, e.g., Ref. 9). It has been necessary to concentrate here specifically on
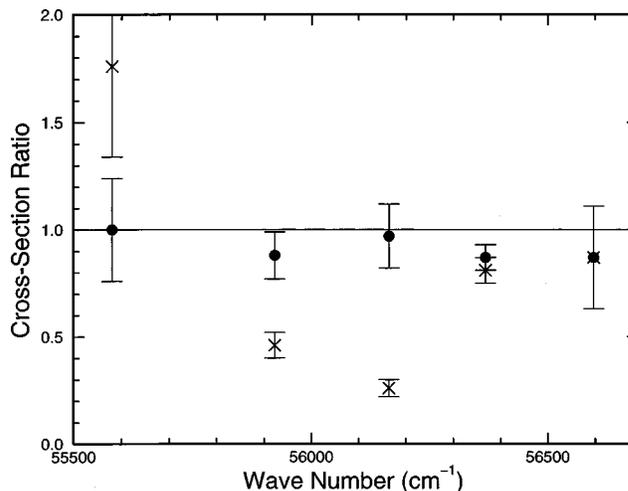

FIG. 5. Comparison between CSE and line-by-line model (Refs. 8, 23) predictions and experimental values of SR cross sections at deepest windows between bands in the (11,0)–(16,0) region. The data, taken from Fig. 4, are plotted as ratios of the model and experimental cross sections. Solid circles: CSE model:experimental. Crosses: line-by-line model:experimental. Error bars reflect only the experimental uncertainties.

the weakly absorbing window regions at very low temperature in order to demonstrate the existence of the quantum-mechanical effects excluded from the line-by-line models. Finally, we emphasize that the above comparisons concern specifically the *discrete* part of the SR system, the present results not being intended to be used directly in atmospheric-modelling applications, which must, inevitably, address the issue of the underlying continuum in a coherent fashion.[22] It seems clear, however, that a CSE-based treatment of the SR bands will form the basis of a superior atmospheric model.

V. CONCLUSIONS

Laser-based measurements of Schumann-Runge photo-absorption cross sections in the weakly absorbing windows between the (11,0) and (16,0) bands have been performed at liquid-nitrogen temperature and the results compared with corresponding coupled-channel Schrödinger-equation and line-by-line model calculations. The excellent agreement found between the CSE and experimental window cross sections serves to confirm the CSE-model predictions of band shape asymmetry and quantum-mechanical interference effects, especially in the (11,0)–(14,0)-band region. On the other hand, the symmetric-line-shape-based line-by-line model cross sections display significant systematic differences from both the experimental and CSE window cross sections. This work provides the first clear evidence for band-shape asymmetry and interference effects in the SR system, which is of significant fundamental interest.

ACKNOWLEDGMENTS

[1] P. M. Dooley, B. R. Lewis, S. T. Gibson, K. G. H. Baldwin, P. C. Cosby, J. L. Price, R. A. Copeland, T. G. Slanger, A. P. Thorne, J. E. Murray, and K. Yoshino, J. Chem. Phys. **109**, 3856 (1998).

[2] P. M. Dooley, Ph. D. thesis, Australian National University, 1997.

[3] T. M. Fang, S. C. Wofsy, and A. Dalgarno, Planet. Space Sci. **22**, 413 (1974).

[4] A. J. Blake, J. Geophys. Res. **84**, 3272 (1979).

[5] M. Allen and J. E. Frederick, J. Atmos. Sci. **39**, 2066 (1982).

[6] D. P. Murtagh, Planet. Space Sci. **36**, 819 (1988).

[7] M. Nicolet and R. Kennes, Planet. Space Sci. **37**, 459 (1989).

[8] K. Minschwaner, G. P. Anderson, L. A. Hall, and K. Yoshino, J. Geophys. Res. **97**, 10103 (1992).

[9] B. R. Lewis, S. T. Gibson, L. W. Torop, and D. G. McCoy, Geophys. Res. Lett. **25**, 2457 (1998).

[10] F. T. Hawes, L. W. Torop, B. R. Lewis, and S. T. Gibson, Phys. Rev. A **63**, 012513 (2000).

[11] K. Minschwaner and V. Starke, Phys. Chem. Earth **C26**, 539 (2001).

[12] B. R. Lewis, P. M. Dooley, J. P. England, K. Waring, S. T. Gibson, and K. G. H. Baldwin, Phys. Rev. A **54**, 3923 (1996).

[13] K. Yoshino, D. E. Freeman, and W. H. Parkinson, J. Phys. Chem. Ref. Data **13**, 207 (1983).

[14] B. R. Lewis, S. T. Gibson, F. T. Hawes, and L. W. Torop, Phys. Chem. Earth **C26**, 519 (2001).

[15] E. F. van Dishoeck, M. C. van Hemert, A. C. Allison, and A. Dalgarno, J. Chem. Phys. **81**, 5709 (1984).

[16] L. Torop, D. G. McCoy, A. J. Blake, J. Wang, and T. Scholz, J. Quant. Spectrosc. Radiat. Transf. **38**, 9 (1987).

[17] In contrast to line-by-line SR models, where an additional full set of parameters is required for each isotopomer, no further parameters are required for the CSE model, the isotopic cross section being computed simply by changing the reduced mass in the relevant equations (see Ref. 14).

[18] S. T. Gibson, B. R. Lewis, K. G. H. Baldwin, and J. H. Carver, J. Chem. Phys. **94**, 1060 (1991).

[19] B. R. Lewis, S. T. Gibson, and E. H. Roberts, J. Chem. Phys. **115**, 245 (2001).

[20] B. R. Lewis, S. T. Gibson, and P. M. Dooley, J. Chem. Phys. **100**, 7012 (1994).

[21] B. R. Lewis, L. Berzins, J. H. Carver, S. T. Gibson, and D. G. McCoy, J. Quant. Spectrosc. Radiat. Transf. **34**, 405 (1985).

[22] The non-SR continuum is due to the Herzberg transitions, together with transitions into $^3\Pi_u$ and $^3\Pi_g$ states. In the context of atmospheric applications requiring SR-region modeling, this continuum is usually defined as the difference between the experimental cross section and the SR-band contribution. Since this model-dependent definition is clearly inappropriate for the comparisons examined here, we rely on a computed continuum cross section informed by SR-independent experimental data (see Ref. 19).

[23] K. Minschwaner (private communication).

[24] The line-by-line cross sections also *exclude* the effects of the SR continuum, but at 79 K this continuum is insignificant ($<10^{-23}$ cm^2) over the full range of transition energies studied here.

[25] K. Yoshino, D. E. Freeman, J. R. Esmond, and W. H. Parkinson, Planet. Space Sci. **35**, 1067 (1987).

[26] The high-energy points in Fig. 5 near 56 597 cm^{-1} are the most uncertain. The corresponding scanned experimental cross section is significantly lower than the fixed-wavelength measurement of Fig. 2(a), possibly caused by the very narrow minimum in the cross section, together with some wavelength uncertainty. Furthermore, the CSE model suffers from some systematic line position errors in this high-energy, perturbed region of the spectrum, as evident in Fig. 4(e). The plotted points are determined using the minimum experimental and model cross sections in this region, regardless of exact wavelength.